A Finite-State Markov Chain Model for Statistical Loss Across a RED Queue

Mohit B. Singh Homayoun Yousefi'zadeh Hamid Jafarkhani
Department of Electrical Engineering and Computer Science
University of California, Irvine
[msingh,hyousefi,hamidj]@uci.edu

***Abstract*— In this paper, we present an analytical study targeted at statistically capturing the loss behavior of a RED queue. We utilize a finite-state Markov chain model. Starting from recursive equations of the model, we derive equivalent closed-form equations. We numerically validate the matching of recursive and closed-form equations. Further, we apply our model to monitor the average RED queue size in a number of sample topologies illustrating their practicality. Based on our results, we argue that our model can adapt to the changing network conditions.**

***Index Terms*—RED, Markov Chain, Packet Loss Modeling.**

I. Introduction

Identifying effective congestion and flow control schemes for both TCP and UDP has been an active area of research in the past decade. In the recent years, a number of proposed schemes have made way into implementations [9]. Nonetheless, high flow loss rate remains to be a challenging problem for congested networks. One of the reasons of the high loss rate, is the failure of the network to provide early congestion notification to the traffic sources. This has led Internet Engineering Task Force (IETF) to recommend the use of active queue management algorithms [2] including random drop [6], early packet discard [11], and random early drop [7]. The most prominent and widely studied queue management scheme is Random Early Detection (RED) [4]. RED queues alleviate many of the problems found in other active queue management algorithms.

Although RED can potentially outperform traditional drop-tail schemes, it is often difficult to parameterize RED queues under different congestion scenarios. In addition, RED needs constant tuning to adapt to current network conditions. Based on simplified models, guidelines have been proposed in [4], [3], [14] for setting RED parameters. However, most studies on RED are based on heuristics or simulations rather than a systematic approach. Of these, the authors of [1] and [5] have modeled RED stochastically, while those of [8], [13], and [12] have used a Markovian model to study RED.

Most of the recent research has tried to tune the RED parameters, namely, maximum and minimum thresholds, but has not addressed the issue of the optimum shape of the intermediate sub-regime Further, the issue of QoS measured in term of average loss over RED has not been studied adequately. In this paper, we propose a 3-state Markov chain model to capture the dynamics of a RED queue. Starting from the recursive equations of the model, we find the closed-form approximations for them. We do so, by converting the model to an equivalent 2-state model. This model can be used to characterize the loss behavior of a RED gateway, or alternatively that of end-to-end UDP or TCP traffic passing through RED gateways.

This paper is structured as follows: In Section 2, we present a 3-state Markov chain model for RED and derive the recursive equations representing it. In Section 3, we derive approximated closed-form solutions for the model by means of applying a number of finite-state Markov chain transformations. In Section 4, we present simulation results supporting the equivalence of the transformations. We also present simulation results of applying our model to a number of sample topologies utilizing NS2 [17]. Finally, we present concluding remarks and future work in Section 5.

II. Markov Modeling of RED

The average queue size of a RED queue is calculated using a low-pass filter with an exponential weighted moving average as

$$q_t \leftarrow (1 - w_q)q_{t-1} + w_q * \tilde{q}_t \tag{1}$$

where q_t is the current average queue size, q_{t-1} is the average queue size at the last time instant, w_q is the queue weight, and $\tilde{q}_t$ is the current queue size. q_t is then compared to two thresholds, a minimum threshold q_{min} and a maximum threshold q_{max}. Each arriving packet is marked with probability p given by

$$p = \begin{cases} 0 & \text{if} \quad q_t < q_{min} \\ \frac{q - q_{min}}{q_{max} - q_{min}}\, p_{max} & \text{if} \quad q_{min} \le q_t < q_{max} \\ 1 & \text{if} \quad q_t \ge q_{max} \end{cases} \tag{2}$$

In Equation (2), p is varied linearly from 0 to p_{max} in the region between q_{min} and q_{max}. There are many possibilities of choosing this drop probability as a linear or non-linear, convex or concave function of queue size. Selecting this intermediate sub-regime impacts the performance of RED.

The temporally correlated loss observed in the Internet due to the drop-tail queues can be modeled by the 2-state Gilbert loss model [15]. In the Gilbert model, a state G known as the GOOD state represents the receipt of a packet and a state B known as the BAD state represents the loss of a packet. State G introduces a probability $P_G = \gamma$ of staying in state G and $1 - P_G$ of transitioning to state B. State B introduces a probability $P_B = \beta$ of staying in state B and $1 - P_B$ of transitioning to state G.

As shown in Fig. 1, we introduce one more state I to which we refer as the INTERMEDIATE state for the modeling of RED. This is a state representing a packet loss probability of p with $0 < p < 1$. Thus, we model a RED queue as a 3-state Markov chain with states G, B, and I corresponding to

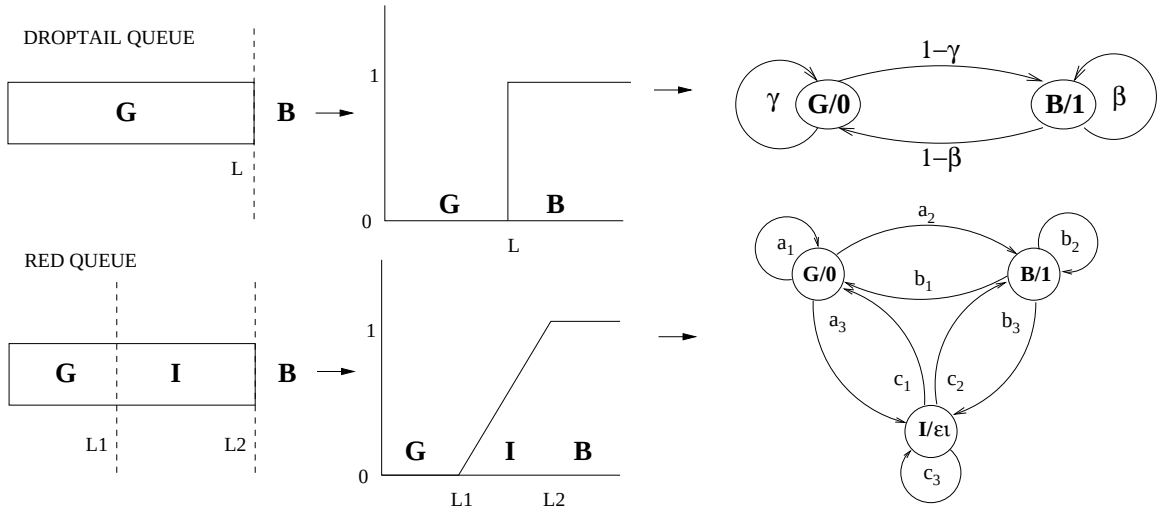

Fig. 1. Markov modeling of a drop-tail queue and a RED queue with $p_{max} = 1$.

the cases when the queue is below q_{min}, above q_{max}, and between q_{min} and q_{max}. Note that the drop probability in state I is not a number. Rather, it is a random variable denoted by ϵ_i.

Next, we define the transition probabilities of our 3-state model. Let a_1, a_2, a_3 be the probabilities of transitioning from state G to state G, B, I, respectively. Similarly, let b_1, b_2, b_3 and c_1, c_2, c_3 be the probabilities of transitioning from state B to G, B, I and from state I to G, B, I, respectively. Note that a_3 = (1-a_1-a_2), b_3 = (1-b_1-b_2), and c_3= (1- c_1-c_2). Let $P(u, v)$ be the probability of keeping v packets from u arrived packets. Further, let $P(u, v, G)$, $P(u, v, B)$, and $P(u, v, I)$ be the probabilities of keeping v packets from u arrived packets and ending up in states G, B, and I, respectively. We can use the following recursive equations to find $P(u, v)$ for any u and v as

$$\begin{aligned}
P(u,v,G) &= P(u-1,v-1,G)a_1 + P(u-1,v-1,B)b_1 \\
&\quad + P(u-1,v-1,I)c_1 \\
P(u,v,B) &= P(u-1,v,G)a_2 + P(u-1,v,B)b_2 \\
&\quad + P(u-1,v,I)c_2 \\
P(u,v,I) &= \{P(u-1,v-1,G)a_3 + P(u-1,v-1,B)b_3 \\
&\quad + P(u-1,v-1,I)c_3\}(1-\epsilon_i) + \{P(u-1,v,G)a_3 + \\
&\quad P(u-1,v,B)b_3 + P(u-1,v,I)c_3\}\epsilon_i \\
P(u,v) &= P(u,v,G) + P(u,v,B) + P(u,v,I)
\end{aligned} \tag{3}$$

III. Closed-Form Solutions of the RED Markov Model

In this section, we derive closed-form solutions for $P(u, v)$ starting from recursive equations of (3).

In [15], a similar analysis for the Gilbert model is carried out. The closed-form solutions for the 2-state Gilbert model are given as

$$\begin{aligned}
&P(v+z, v, G) = \\
&\quad \gamma^{v-z}\,(1-\beta)\,(1-\gamma)\,\{ \\
&\quad\quad \textstyle\sum_{i=0}^{z-1} \binom{z-1}{i}\binom{v}{i+1}(\beta\,\gamma)^{z-1-i}\,[(1-\beta)\,(1-\gamma)]^i \\
&\quad \}\,G_{ss} \quad + \quad \gamma^{v-z-1}\,(1-\beta)\,\{ \\
&\quad\quad \textstyle\sum_{i=0}^{z} \binom{z}{i}\binom{v-1}{i}(\beta\,\gamma)^{z-i}\,[(1-\beta)\,(1-\gamma)]^i \\
&\quad \}\,B_{ss} \qquad\qquad z \geq 1\,,\; v \geq z+1
\end{aligned} \tag{4}$$

and

$$\begin{aligned}
&P(v+z, v, B) = \\
&\quad \gamma^{v-z+1}\,(1-\gamma)\,\{ \\
&\quad\quad \textstyle\sum_{i=0}^{z-1} \binom{z-1}{i}\binom{v}{i}(\beta\,\gamma)^{z-1-i}\,[(1-\beta)\,(1-\gamma)]^i \\
&\quad \}\,G_{ss} \quad + \quad \gamma^{v-z}\,(1-\beta)\,(1-\gamma)\,\{ \\
&\quad\quad \textstyle\sum_{i=0}^{z-1} \binom{z}{i+1}\binom{v-1}{i}(\beta\,\gamma)^{z-1-i}\,[(1-\beta)\,(1-\gamma)]^i \\
&\quad \}\,B_{ss} \qquad\qquad z \geq 1\,,\; v \geq z
\end{aligned} \tag{5}$$

where $u = v + z$. However, obtaining closed-form solutions of the 3-state RED model is more complicated than that of the 2-state Gilbert model. The Gilbert model contains just 2 possible transitions and 2 trivial drop probabilities, while the 3-state RED model contains 9 possible transitions and a pair of trivial drop probabilities along with a drop probability which is a random variable. Considering the complexity of the problem, we transform the model as illustrated in Fig. 2. First, we split state I into 2 states, namely, I^g (Intermediate GOOD) and I^b (Intermediate BAD), with the characteristic that the drop probabilities in these states are not random numbers. Rather, they are 0 and 1 respectively. However, our transition probabilities containing the term ϵ_i are random. We rename the transition probabilities of our resulting 4-state model for the ease of convention as shown in Fig. 2.

Next, we observe that the drop probability is 0 in G or I^g and 1 in B or I^b. Thus, we merge these states to reduce our model to a 2-state model as shown in Fig. 2. The resulting model is not a deterministic Gilbert model since the transition probabilities of the resulting model are random. Nonetheless, we can still use the closed-form expressions of (4) and (5), albeit that

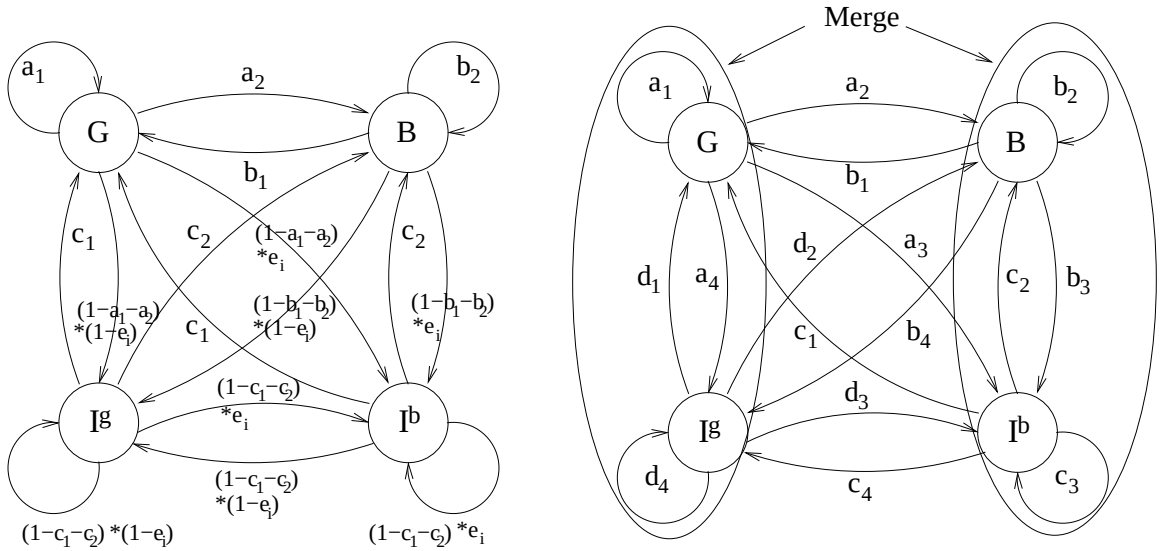

Fig. 2. The 4-state model and pairwise classification of its states.

our $P(u,v)$ would be a random variable rather than a deterministic value. We need to express γ and β of the resulting model in terms of the 3-state model parameters, to form closed-form solutions of the RED queue.

We note that γ is the probability of starting from $P(u-1,v-1,G)$ and going to $P(u,v,G)$ for the transformed 2-state model. To find γ, we need $P(u-1,v-1,G)$ and $P(u-1,v-1,I^g)$ for each u and v of the 4-state model. Although we have the sum of these two quantities as the $P(u,v,G)$ of the 2-state model, we do not have the individual terms as the result of combining the states.

Assuming the 4-state model is in the steady-state and for large u and v, we can approximate the ratio of the probability of being in G and the probability of being in I^g by the ratio of their steady-state probabilities G_{ss} and I^g_{ss}. This gives

$$\begin{aligned} P(u,v,G)\gamma &= P(u-1,v-1,G)[\tfrac{G_{ss}}{G_{ss}+I^g_{ss}}(a_1+a_4) \\ &\quad +\tfrac{I^g_{ss}}{G_{ss}+I^g_{ss}}(d_1+d_4)] \\ \gamma &= \left[\tfrac{G_{ss}}{G_{ss}+I^g_{ss}}(a_1+a_4)+\tfrac{I^g_{ss}}{G_{ss}+I^g_{ss}}(d_1+d_4)\right] \end{aligned} \tag{6}$$

A similar analysis applies to β, with I^b_{ss} and B_{ss} as steady-state probabilities of being in I^b and B. We use equilibrium equations to get G_{ss}, I^g_{ss}, B_{ss} and I^b_{ss} as follows:

$$\begin{aligned} G_{ss} &= a_1G_{ss}+b_1B_{ss}+c_1I^b_{ss}+d_1I^g_{ss} \\ B_{ss} &= a_2G_{ss}+b_2B_{ss}+c_2I^b_{ss}+d_2I^g_{ss} \\ I^b_{ss} &= a_3G_{ss}+b_3B_{ss}+c_3I^b_{ss}+d_3I^g_{ss} \\ I^g_{ss} &= a_4G_{ss}+b_4B_{ss}+c_4I^b_{ss}+d_4I^g_{ss} \end{aligned} \tag{7}$$

While only 3 of the above equations are linearly independent, we can extract a 4-th equation from the probability of the sum to express:

$$\begin{aligned} (1-a_1)G_{ss}+b_1B_{ss}+c_1I^b_{ss}+d_1I^g_{ss} &= 0 \\ a_2G_{ss}+(1-b_2)B_{ss}+c_2I^b_{ss}+d_2I^g_{ss} &= 0 \\ a_3G_{ss}+b_3B_{ss}+(1-c_3)I^b_{ss}+d_3I^g_{ss} &= 0 \\ G_{ss}+B_{ss}+I^b_{ss}+I^g_{ss} &= 1 \end{aligned} \tag{8}$$

The solution of this system of linear equations is given by

$$G_{ss}=\frac{\Delta_1}{\Delta};B_{ss}=\frac{\Delta_2}{\Delta};I^b_{ss}=\frac{\Delta_3}{\Delta};I^g_{ss}=\frac{\Delta_4}{\Delta} \tag{9}$$

Further simplification occurs because $c_1 = d_1$, $c_2 = d_2$, $c_3 = d_3$, $c_4 = d_4$, and $a_3/a_4 = b_3/b_4 = c_3/c_4 = d_3/d_4$. These constraints are obtained because we start from a 3-state model and convert it to a 4-state model. The resulting 4-state model does not have all possible combinations of the transition probabilities. As a result, we get

$$\begin{aligned} \Delta_1 &= -\begin{vmatrix} b_1 & c_1 & 0 \\ (b_2\text{-}1) & c_2 & 0 \\ b_3 & (c_3\text{-}1) & 1 \end{vmatrix} \\ \Delta_2 &= \begin{vmatrix} (a_1\text{-}1) & c_1 & 0 \\ a_2 & c_2 & 0 \\ a_3 & (c_3\text{-}1) & 1 \end{vmatrix} \\ \Delta_3 &= -\begin{vmatrix} (a_1\text{-}1) & b_1 & c_1 \\ a_2 & (b_2\text{-}1) & c_2 \\ a_3 & b_3 & c_3 \end{vmatrix} \\ \Delta_4 &= \begin{vmatrix} (a_1\text{-}1) & b_1 & c_1 \\ a_2 & (b_2\text{-}1) & c_2 \\ a_3 & b_3 & (c_3\text{-}1) \end{vmatrix} \\ \Delta &= \begin{vmatrix} (a_1\text{-}1) & b_1 & c_1 \\ a_2 & (b_2\text{-}1) & c_2 \\ 1 & 1 & 1 \end{vmatrix} \\ &= \Delta_1+\Delta_2+\Delta_3+\Delta_4 \end{aligned} \tag{10}$$

IV. Numerical Validation

A. Results Comparing 2-State and 3-State Markov Models

For examining our approximation, we choose a set of 3-state model parameters and find the equivalent 2-state parameters.

Then, we compare $P(v+z,v)$ with $z \leq v$ over different ranges of parameter v. From the sets of experiments conducted by us, we select two ranges of parameter v, namely, $v \in [1,20]$ and $v \in [90,100]$. Fig. 3 (a) and (b) show the results of those two experiments, respectively. The values of $P(v+z,v)$ obtained differ very slightly for most values of v. In addition, the slight mismatch decreases with increasing v. This shows that the Markov chain quickly moves toward and stays in equilibrium validating the approximation.

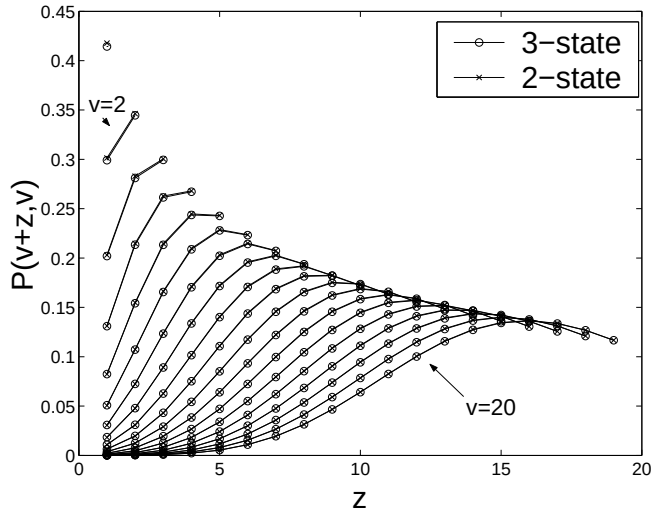

(a)

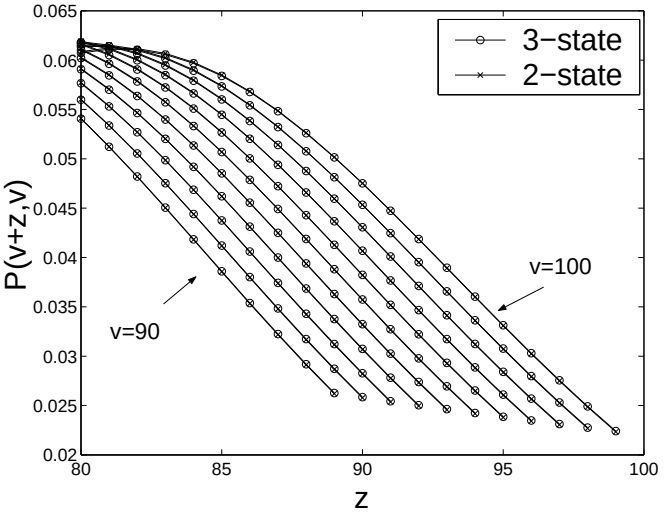

(b)

Fig. 3. (a) $P(v+z,v)$ for $v \in [1,20]$, and (b) $P(v+z,v)$ for $v \in [90,100]$.

B. NS2 Experiments

In this section, we provide simple ways of measuring the parameters of our model in RED queus utilizing their statistical properties. We utilize two simulation topologies shown in Fig 4. The first topology to which we refer as the 4-flow topology, is a half-dumbbell topology with 4 TCP/FTP sources transmitting to a sink. The second topology to which we refer as the 3-flow topology, is a full-dumbbell topology with 3 TCP/FTP sources transmitting to 3 different sinks. We set up the simulation parameters such that the TCP links always operate at the maximum possible data rate allowed by the bottleneck link. The link bandwidths and delays are shown in Fig. 4 (a) and (b). For each topology, we experiment with different bottleneck link bandwidths.

The plots displayed in Fig. 4 (c) and (d), are the plots of instantaneous queue size ($\tilde{q}_t$) and average queue size (q_t) for a RED queue with $w_q = 0.002$. Since RED uses q_t to evaluate drop probabilities, we use the same quantity to extract the transition probabilities and steady-state probabilities for our 3-state model. In order to obtain transition probabilities, we count all of the transitions of q_t from I, G, or B to I, G, or B, and divide them by the total number of transitions. Here, $q_t < q_{min}$ represents the G region, $q_{min} \leq q_t < q_{max}$ represents the I region, and $q_t \geq q_{max}$ represents the B region. We note that anytime $\tilde{q}_t$ reaches q_{max}, all subsequent packets are dropped. The latter is due to the fact that the size of the queue is the same as q_{max}, and hence the transition is counted as one going to the B state. Similarly, the total number of times the queue is in I, G, and B states divided by the total number of times give steady-state probabilities of being in these states.

We have performed simulations for bottleneck link bandwidths ranging from 0.1Mbps to 100Mbps. The number of flows have been varied from 2 to 20 with different values of the queue weight (w_q) for RED. Due to space limitation we do not present all of our results. The simulations show that ϵ_i which directly depends on q_t, resembles a quasi static random variable. Further, its value does not vary much around a mean value. Hence, we use the mean value of ϵ_i to obtain numerical values of the equivalent 2-state transition probabilities.

Table IV-B includes Markov model parameters obtained for 4-flow topology with $w_q = 0.002$. Reviewing the results of Table IV-B reveals that c_3 is the dominant transition probability. The latter validates our modeling approach, as the primary aim of RED is to operate the queue in the I state. The value of c_3 becomes less dominant as we increase the number of flows. This is intuitive, since informing a larger number of sources about the queue state causes a longer delay in controlling the traffic. In fact, the transitions to state B increase as the result of increasing the number of sources. Further, the mean and variance of ϵ_i respectively indicated by μ_{ei} and σ_{ei} increase as the number of sources increase.

We do not observe a large number of transitions to state G

TABLE I

MARKOV MODEL PARAMETERS OBTAINED FOR 4-FLOW TOPOLOGY WITH $w_q - 0.002$.

BW	3-state model params	Eqv. 2-state model params
$3Mbps$	a1=0, a2=0, a3=0, b1=0, b2=0, b3=1,c1=0, c2=0.007, c3=0.993, μ_{ei}=0.055, σ_{ei}=0.00896	g0=0.939, b0=0.062, γ=0.938, β=0.061

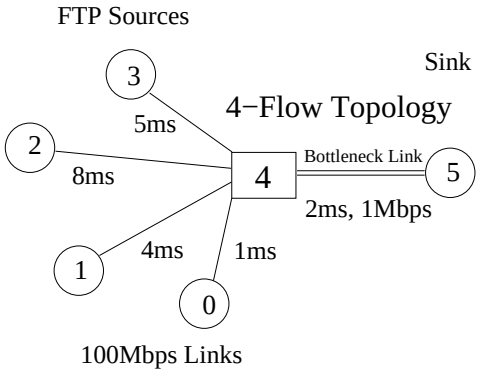

(a)

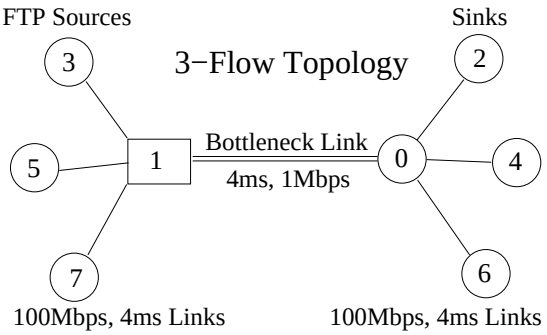

(b)

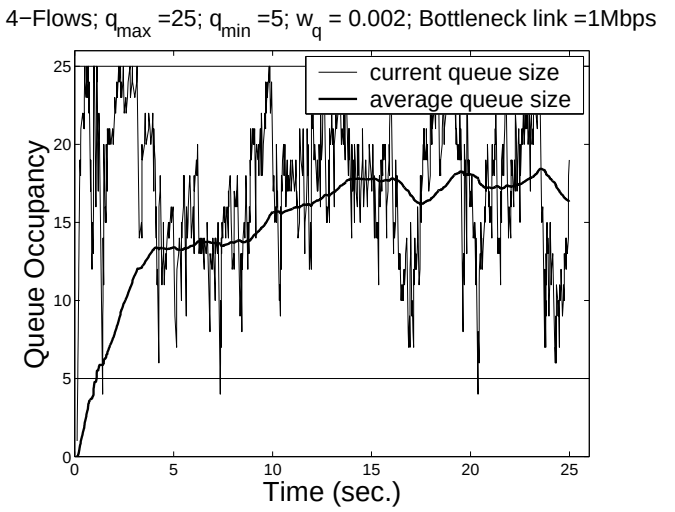

(c)

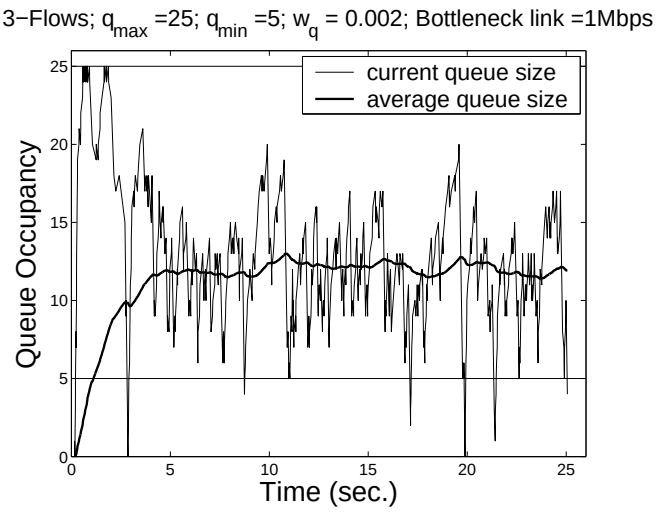

(d)

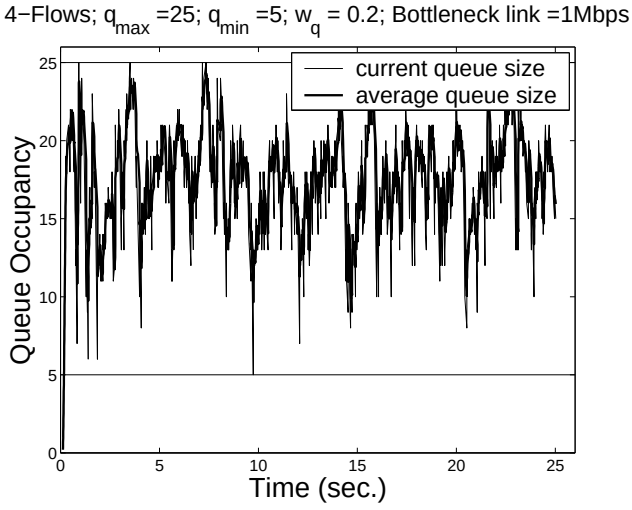

(e)

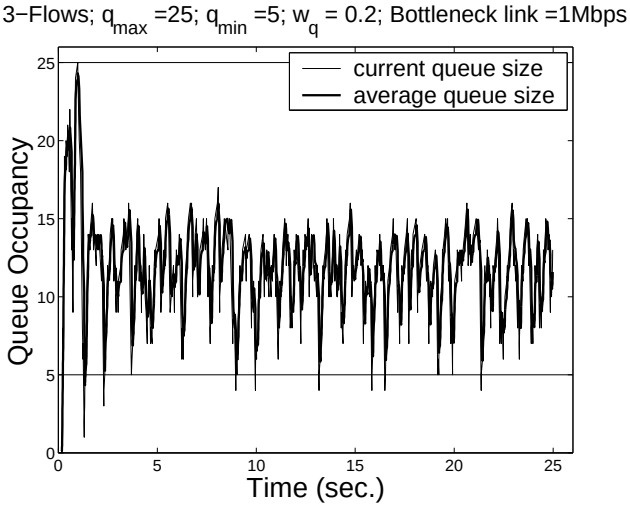

(f)

Fig. 4. (a) 4-flow topology, (b) 3-flow topology, (c) q_t and $\tilde{q_t}$ vs time for 4-flow topology with $w_q = 0.002$, (d) q_t and $\tilde{q_t}$ vs time for 3-flow topology with $w_q = 0.002$, (e) q_t and $\tilde{q_t}$ vs time for 4-flow topology with $w_q = 0.2$, (d) q_t and $\tilde{q_t}$ vs time for 3-flow topology with $w_q = 0.2$.

unless w_q is a large number signifying a smaller averaging window. The plots displayed in Fig. 4 (e) and (f) are similar to those displayed in Fig. 4 (c) and (d) for the choice of $w_q = 0.2$. As observed from the figures, the average queue sizes more closely follow the instantaneous queue sizes for larger values of w_q. We also note that there are more fluctuations in the average queue size as w_q becomes larger.

The values of transition probabilities of our model provide useful insight into conditions at RED gateway. We summarize our findings as follows. More transitions from I to B and I to G are observed if q_{max} and q_{min} are chosen close to each other. The model parameters are determined depending on operating conditions. Of course, I to I transitions would dominate under good operating conditions. Further, we have observed that even for a large w_q, more transitions to state G are occurred for smaller number of sources and narrower width of I region identified by $q_{max} - q_{min}$.

At the end of this section, we note that this model can be easily applied to the changing network conditions by updating the model parameters using a weighted contribution from the newer values of q_t. Additionally, a statistical guarantee algorithm such as the one proposed by our earlier work of [15] can be applied along with this model to provide end-to-end QoS guarantee for the traffic sources accommodated by RED queues. Our work of [16] introduces appropriate UDP end node signaling schemes for such a task.

V. Conclusions

In this paper, we presented a finite-state Markov chain model to capture the dynamics of a RED queue. We found closed-form equations closely approximating the behavior of the RED queue. Further, we validated the results of our modeling task by means of simulations. Utilizing the model, we are investigating optimum representations of the intermediate region between q_{min} and q_{max} for a RED queue accommodating hybrid TCP and UDP flows. The latter reuires capturing the UDP feedback mechanisms in the model another area of our research focus. Further, we are currently in process of creating an end-to-end statistical guarantee algorithm of QoS for RED queues accommodating a mix of TCP and UDP flows. We leave this and developing similar models for other queuing disciplines as a part of our future work.

References

[1] H.M. Alazemi, A. Mokhtar, M. Azizoglu, "Stochastic Approach for Modeling Random Early Detection Gateways in TCP/IP Networks," In Proc. IEEE ICC, 2001.

[2] R. Braden, D. Clark, J. Crowcroft, B. Davie, S. Deering, D. Estric, S. Floyd, V. Jacobson, G. Minshall, C. Petridge, L. Peterson, K. Ramakrishnan, S. Shenker, J. Wroclawski, L. Zhang, "Recommendations on Queue Management and Congestion Avoidance in the Internet," Internet Draft, March 1997.

[3] V. Firoiu, M. Borden, "A Study of Active Queue Management for Congestion Control," In Proc. IEEE INFOCOM, 2000.

[4] S. Floyd, V. Jacobson, "Random Early Detection Gateways for Congestion Avoidance," IEEE/ACM Trans. Networking, August 1993.

[5] L. Guan, I.U. Awan, M. E. Woodward, "Stochastic Modeling of Random Early Detection based Congestion Control Mechanism for Bursty and Correlated Traffic," In Proc. IEE Software 151, October 2004.

[6] E. Hashem, "Analysis of Random Drop for Gateway Congestion Control," MIT Technical Report, 1990.

[7] V. Jacobson, "Presentations to the IETF Performance and Congestion Control Working Group," August 1989.

[8] R. Laalaoua, T. Czachorski, "Markovian Model of RED Mechanism," In Proc. CCGRID, 2001.

[9] S. Ladha, P.D. Amer, A. Caro, J.R. Iyengar, "On the Prevalence and Evaluation of Recent TCP Enhancements," In Proc. IEEE GLOBECOM, 2004.

[10] M. May, T. Bonald, J. Bolot, "Analytic Evaluation of RED Performance," In Proc. IEEE INFOCOM, 2000.

[11] A Romanov, S. Floyd, "Dynamics of TCP Traffic Traffic over ATM networks," In Proc. ACM SIGCOMM, 1994.

[12] S. Suthaharan, "Markov Model Based Congestion Control for TCP," Annual Simulation Symposium, 2004.

[13] Y.C. Wang, J.A. Jiang, R.G. Chu, "Drop Behaviour of Random Early Detection with Discrete-Time Batch Markovian arrival process," In Proc. IEE Software 151, August 2004.

[14] T. Ye, S. Kalyanraman, "Adaptive Tuning of RED Using On-line Simulation," In Proc. IEEE GLOBECOM 2002.

[15] H. Yousefi'zadeh, H. Jafarkhani, "Statistical guarantee of QOS in Communication Networks with Temporally Correlated Loss," In Proc. IEEE GLOBECOM, 2003.

[16] H. Yousefi'zadeh, F. Fazel, H. Jafarkhani, "Hybrid Unicast and Multicast Flow Control: A Linear Optimization Approach," In Proc. IEEE/IEE HSNMC, 2004.

[17] -, "The Network Simulator-NS2," Avilable at http://www.isi.edu/nsnam/ns/.